BOUNDARY LAYER DEVELOPMENT ALONG SMOOTH AND CORRUGATED AIRFOIL SURFACES

H.A. Abdalla, A.M. Alam El-din, T.I. Sabry and S.R. Ismail

Department of Mechanical Power Engineering, Faculty of Engineering,
Menoufia University, Shebin El-Kom, Egypt

ABSTRACT

This paper describes an experimental study of the effects of a sinusoidal corrugation roughness upon the aerodynamic performance and the boundary layer development past a symmetrical airfoil. Corrugation roughness airfoils have been used in advanced gas turbine cooling designs to enhance the internal heat transfer. Effects of corrugation roughness on the lift and drag coefficients as a function of angle of attack, corrugation length and Reynolds number were tested. Measurements of pressure distributions and velocity distributions were carried out at different angles of attack to determine the boundary layer parameters with and without pressure gradients. It is concluded that, the maximum lift-to-drag ratio of corrugated airfoils increases with increasing the Reynolds number and decreases with increasing the length of corrugation. There is evidence of a strong distortion of the downstream turbulent boundary layer. The turbulent boundary layer past corrugated airfoils grows more rapidly and separates earlier than that of smooth airfoil. This is important in assessing the measured characteristics of turbulent boundary layers.

Keywords: Corrugation roughness, Airfoil, Performance, Lift and drag coefficients, Boundary layer, Flow separation.

INTRODUCTION

Turbulent flow past wavy or corrugated boundaries has attracted considerable research attention in recent years. Fluid flowing over the corrugated or wavy surfaces of sinusoidal geometry or arcs of circles experiences large positive and negative pressure gradients. On the other hand, the flow past such surfaces is subjected to the corrugation roughness effects. In this case, the characteristics of turbulent boundary layer depend on a group of parameters such as surface length, fluid velocity, fluid properties and surface geometry. It is well known that, the surface geometry has a considerable effect on the boundary layer growth. Introducing some sources of turbulence represented in stepped and corrugated surfaces affect the characteristics of the boundary layer, due to sudden changes of flow directions which results in flow separation. The expected flow structure in corrugated surfaces give an insight applicable to the design of mass transfer devices using vortex mixing. Such a geometry has also a considerable effect on the heat transfer characteristics in corrugated surfaces and tubes.

There has been an increasing interest in the design and performance of airfoils operating in low Reynolds number flows. This interest has been the result of the desire to obtain better performance for both military and civilian systems. Applications include turbomachines blading and wings. The airfoil performance is strongly dependent on the airfoil drag due to the surface irregularities and the surface roughness. The great majority of the existing work on roughness elements is limited to the flow past a single element. Klebanoff *et al.* [1] studied the flow past a row of elements mounted on a flat plate at zero-pressure gradient and obtained values of the

roughness Reynolds number when transition had just been brought forward to the row. The transition seemed to be affected by a close spacing of the roughness elements, the closer spacing increasing the value of the roughness Reynolds number. However, Carmichael [2] did similar experiments using roughness elements of cylindrical shape and obtained the opposite result. Loftin [3] also did experiments using cylindrical elements but on an airfoil. He found that the value of the Reynolds number of roughness was not sensitive to the spacing of the elements provided this it was greater than three times the roughness diameter. Experimental data was given by Gibbings *et. al.* [4,5] for the boundary layer flow past single roughness trips of spherical shape. Correlations are given for the start and end of transition, for the recovery position and for the effective origin of the turbulent layer. The effects of bulges, hollows and ridges on an airfoil and on a flat plate were studied experimentally by Fage [6]. He developed empirical relations between minimum roughness height, roughness width and transition Reynolds number. Brumby [7] tabulated data on the effect of airfoil roughness on maximum lift coefficient. Bragg and Georgerek [8] and Korkan *et al.* [9] were used simulated rime ice as roughness addition of simulated ice to the leading edge of an airfoil, which includes the operating regime of the model helicopter rotor tip. It was found that, the addition of simulated ice to the leading edge of the airfoil creates premature stall, a considerable reduction in maximum lift coefficient and stall angle of attack. The aerodynamic coefficients of the airfoil with the leading edge generic ice showed little dependence on the Reynolds number range tested. The effect of sand-grain roughness type on the aerodynamic performance and the growth of boundary layer along NACA-0012 airfoil model was investigated by Abdalla, *et al.*[10]. They concluded that the presence of sand - grain roughness causes aerodynamic performance degradation and has a significant parameter in thickening the boundary layer. This boundary layer may later to separate, causing a gradual loss of lift as the separation point moves forward with an increase in the surface roughness and the angle of attack. Recently, results from a wind tunnel study of aerodynamically rough turbulent boundary-layer flow over a sinusoidal surface were presented by Wanmin Gong *et. al* [11]. The waves had a maximum slope (ak) of 0.5 and two surface roughness were used (a is the wave amplitude and $k = 2\pi/\lambda$ is the wave number, where λ is the wave length). The results showed that, for relatively rough surface, the flow separated in the wave troughs while for the relatively smooth surface it generally remained attached. Over the relatively smooth surface waves an organized secondary flow developed, consisting of vortex pairs of a scale comparable to the boundary layer depth and aligned with the mean flow. Large-eddy simulation results are also presented.

In some applications such as gas turbine airfoil cooling design, corrugated roughness or repeated rib rough elements have been used to enhance the internal heat transfer, in order to remove more heat from airfoil surfaces exposed to the hot gases [12]. As noted from the previous discussion, there is a few data regarding the change in the aerodynamic performance when the roughness elements are added to an airfoil surface. In addition, the effects of corrugation roughness type on the aerodynamic performance and boundary layer development are not clarified, especially in the presence of pressure gradients. Then, to clarify the effects of corrugation roughness on the aerodynamic performance and flow characteristics, an experimental study of flow over corrugated airfoils at different angles of attack is considered.

NACA-0012 AIRFOIL EXPERIMENT

Wind tunnel tests were conducted with a two-dimensional NACA-0012 airfoils having a corrugated surfaces. The NACA-0012 airfoil evaluated has a chord of 100 mm and 300 mm span. The smooth airfoil surface is made of a filled epoxy resin with the same

chord and span dimensions. The corrugated surface of airfoils are designed and fabricated according to sinusoidal wave shape. The corrugations are made perpendicular to the streamwise direction with a depth d = 1.5 mm and a pitch S = 10 mm. Two corrugated airfoils are fabricated with different corrugated lengths. The corrugated lengths are 50 and 100 percent of the airfoil chord. The geometries of the corrugated airfoils are shown in Figure 1 and Figure 2, which are CS1 and CS2. Static pressure tapping are drilled perpendicular to the airfoil surface with 1 mm diameter. The taps are distributed at the corrugated airfoil chord as shown in Figures 1 and 2.

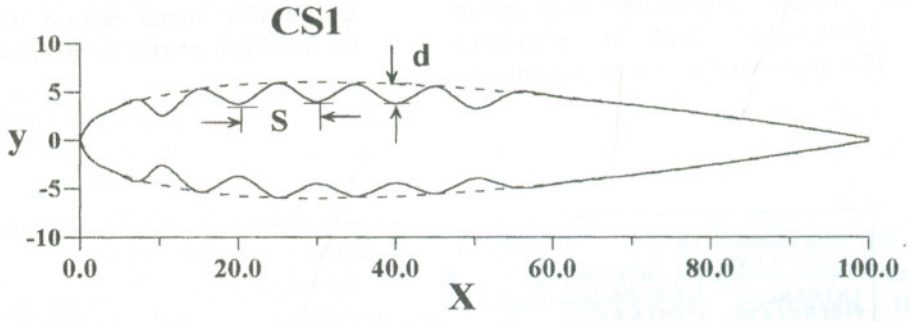

Tap No.	1	2	3	4	5	6	7	8	9	10	11	12	13	14
Position (x/c %)	5	10	15	20	25	30	35	40	45	50	60	70	80	90

Figure 1 Geometry of half corrugated length of NACA-0012 airfoil

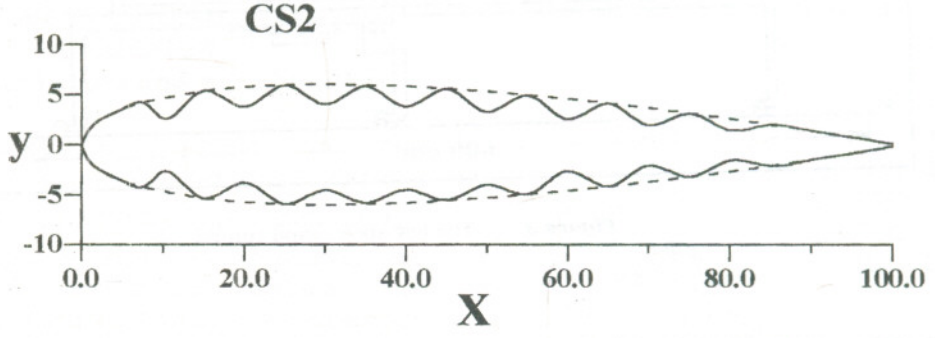

Tap No.	1	2	3	4	5	6	7	8	9	10	11	12	13	14	15	16	17	18
Position (x/c %)	5	10	15	20	25	30	35	40	45	50	55	60	65	70	75	80	85	90

Figure 2 Geometry of full corrugated length of NACA-0012 airfoil

EXPERIMENTAL FACILITIES

The experiments were carried out in a low turbulence open - type wind tunnel. The wind tunnel employed in these experiments is shown in Figure 3. It consists of six parts centeraxial fan, wide angle diffuser, test section, contraction with 0.25 to 1.0 diameter ratio, settling chamber and the entrance portion. All the wind tunnel, except the fan, is made of fiberglass and fixed on a movable steel frame. Honeycomb and graduated screens are

installed in the settling chamber of breaking the free-stream turbulence which is less than 0.05 % at air velocity of 55 m/s. The control panel of the wind tunnel consists of a variable frequency controller and a remote speed control device. The air speed in the test section can be controlled from the control panel of the wind tunnel using a pre-calibrated curve. Calibration for the wind tunnel air speed against the frequency of the wind tunnel controller was made using a pitot-tube and a pressure transducer. The pressure was converted into speed and a straight line relation between the air speed and the frequency was obtained. The test section, which is made of prespex, has a square cross-section 305x305 mm and 610 mm long. At the top wall of the test section, a traversing unit was mounted and a small slot in the longitudinal direction was made to accommodate the probe holder. The airfoil model is horizontally mounted by a vertical adjustable strut which allows the airfoil to be inclined at the desired angle of attack.

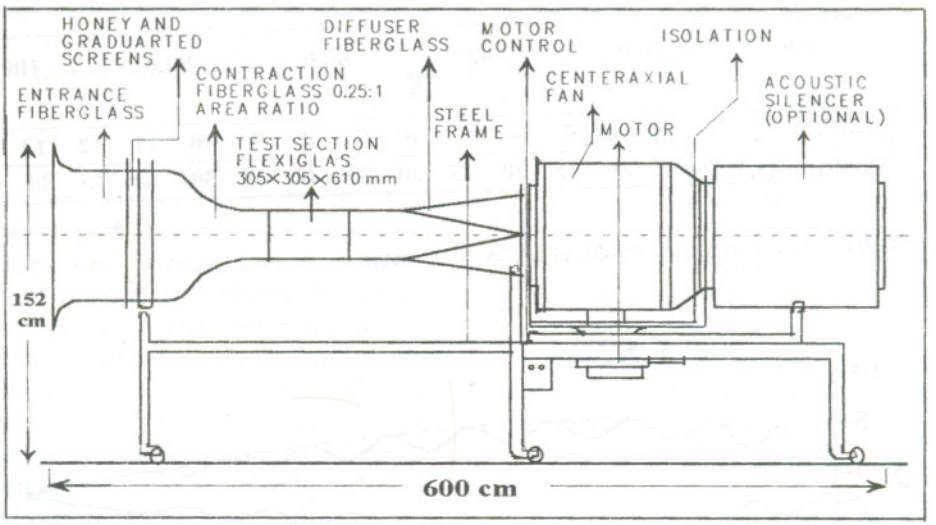

Figure 3 The low speed wind tunnel

Measurements were acquired velocity-profiles in the streamwise direction at angle of attack of 0 and 10 degrees for smooth and corrugated airfoils. A calibrated five-holes probe of 5 mm diameter was used to measure the boundary layer mean velocity profiles along the airfoil chord. The boundary layer momentum thickness, θ, and the displacement thickness, δ^*, as well as the shape factors, H, were obtained from the measured velocity profiles at different locations past the tested airfoils. The chordwise static pressure distributions were measured using sensitive pressure transducers. Beside the boundary layer parameters, the aerodynamic characteristics of the tested models were measured at different angles of attack. The lift and drag forces which give the airfoil performance were measured using the calibrated lift and drag dynamometer. The measurements of mean-velocity profiles are conducted at Reynolds number of 2.02×10^5, while the measurements of pressure distribution, lift and drag coefficients are carried out at different Reynolds number, Re= 2.02×10^5

to 3.37 x 10^5. The Reynolds number is based on the free-stream velocity and the airfoil chord.

The experimental errors in the measurements were calculated using Kline and Mcclintock technique [13]. It was found that, the error in the mean velocity measurements to be in the range of ± 1% at the maximum calibration velocity of 50 m/s. The error in the measured static pressure is about ± 0.5%.

NACA-0012 AIRFOIL AERODYNAMIC PERFORMANCE

The NACA-0012 airfoil section was initially tested with no-corrugation to obtain baseline data and establish agreement with previous studies, [14]. The test of corrugated airfoil surfaces were repeated. Effects on the lift and drag as a function of angle of attack and Reynolds number were then tested to determine aerodynamic increments due to the presence of corrugations. In addition, the growth of boundary layers as well as the flow characteristics were obtained.

EXPERIMENTAL RESULTS AND DISCUSSION

Pressure Distribution and Aerodynamic Performance

A representative sample of the pressure coefficient,Cp, which is defined as $Cp = (P - P_o) / (0.5 \rho U_o^2)$, data on the upper surface of NACA-0012 airfoil with smooth and corrugated surfaces are presented in Figures 4 to 6. The results are plotted at angles of attack of 0.5 and 10 degrees and for Reynolds number of 2.02×10^5. An important feature of these data is the effect of corrugation on the inflection point, the minimum pressure point at which transition to turbulent flow occurs. For zero angle of attack, Figure 4 indicates that the minimum pressure point of the pressure distribution along the upper surface of smooth airfoil is shown at about 20 percent of the chord. This location is the beginning of the creation of adverse pressure gradient. On the other hand, the beginning of the adverse pressure gradient past the upper surface of CS1 and CS2 airfoils is very close to the leading edges, as shown in Figures 5 and 6. In general, the pressure distribution past corrugated airfoils is shown as a step-like distribution in the corrugated regions. The pressure drop along the corrugated airfoils is larger than that of the smooth airfoil. This may be attributed to sudden change of flow directions results in flow separation and the formation of eddy currents that increase the pressure drop. It is observed from Figure 6 that, at 10 degrees angle of attack, the pressure distributions of corrugated airfoil surfaces become approximately flat at X/C=60 percent of the chord up to the trailing edges. This may be attributed to that, as the angle of attack and the section lift coefficient increases, the minimum pressure coefficient decreases. The adverse pressure gradient that results as the flow decelerates toward the trailing edge increases. When the air particles in the boundary layer, already slowed by viscous action, encounter the relatively strong adverse pressure gradient, the boundary layer thickens and separates.

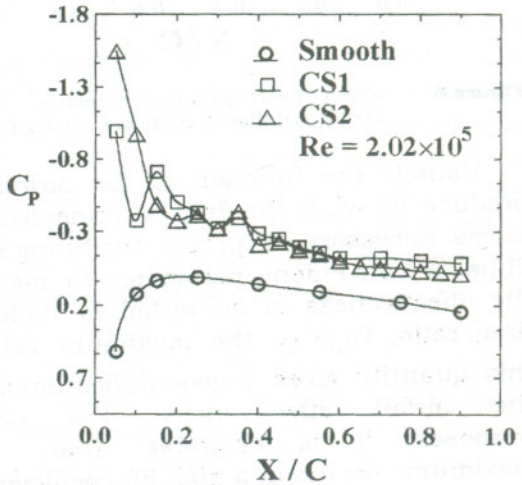

Figure 4 Effect of corrugation on pressure coefficient distribution (α = 0 deg.)

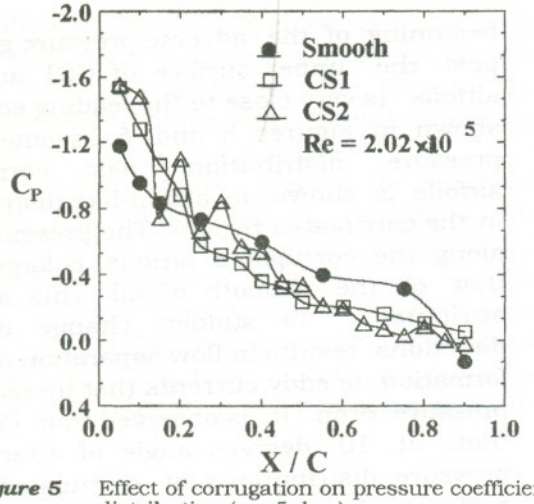

Figure 5 Effect of corrugation on pressure coefficient distribution (α = 5 deg.)

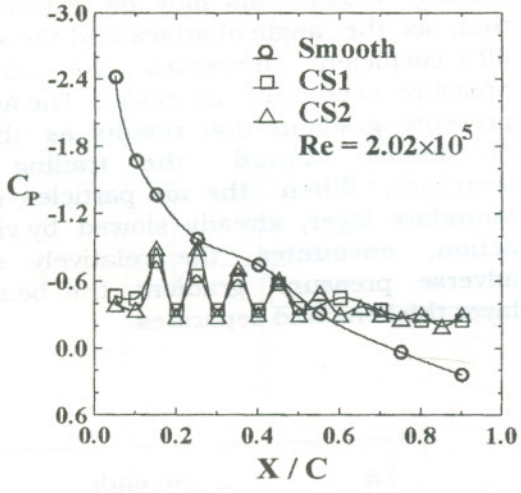

Figure 6 Effect of corrugation on pressure coefficient distribution (α = 10 deg.)

Usually the function of the airfoil is to produce lift while the drag is connected with forces necessary to propel the lifting force. Thus, a convenient parameter to measure the effectiveness of an airfoil is its lift-to-drag ratio, C_L/C_D, the maximum value of this quantity gives a good indication about the airfoil effectiveness. For design purposes, it is desirable that, this maximum occurs at a high lift coefficient so that the physical size of the lifting surface is minimize. The maximum value of C_L which occurs just prior to the flow separation past the airfoil, is denoted by $C_{L\,max}$. The value of angle of attack when lift equal a maximum value is known as the critical angle of attack, α_{cr}. Figures 7 to 9 show the variation of the lift - to - drag ratio of corrugated airfoil compared with the ratio of the smooth airfoil. In these figures, the results of the lift - to - drag ratio are plotted against the angle of attack for different Reynolds number. It can be noticed from these figures that, the maximum lift -to - drag ratios of corrugated airfoil are shown to be lower than that of smooth airfoil. This occurs due to the increase in the drag coefficient for the corrugated airfoil configurations. When there is no appreciable separation of the flow, the drag on the airfoil is caused primarily by skin friction. Thus, the value of the drag coefficient depends on the relative extent of the laminar boundary layer. A sharp increase in the drag coefficient results when transition is shifted toward. If the airfoil surface is sufficiently rough to cause transition near the airfoil leading edge, large increases in drag are obtained. In addition, increases the length of corrugation accompanied by an increase in the airfoil drag which lowered the value of this parameter. Consequently, the critical angle of attack (α_{cr}) at which the maximum lift - to - drag ratio occurs is decreased with increasing the length of corrugation.

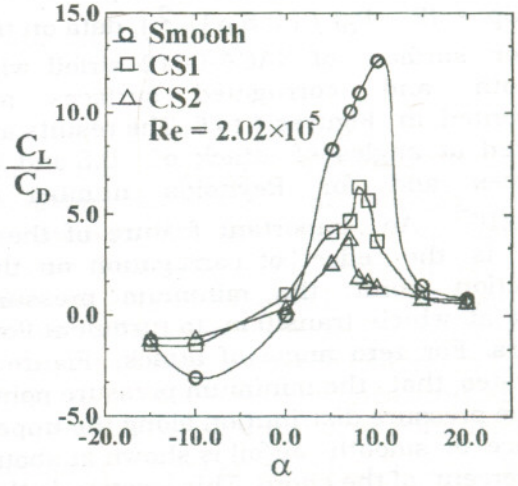

Figure 7 Liff-to-drag ratio of smooth and corrugated airfoils with attack angle

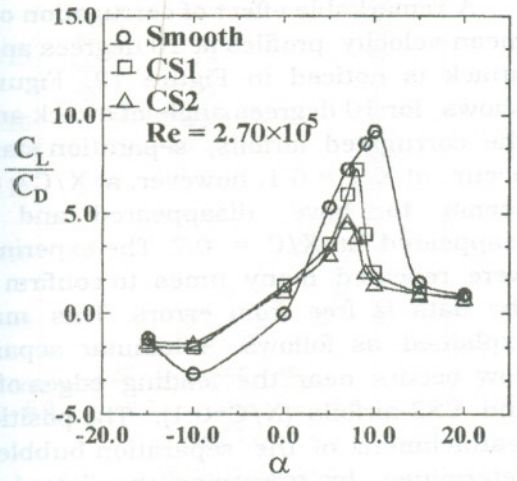

Figure 8 Lift-to-drag ratio of smooth and corrugated airfoils with attack angle

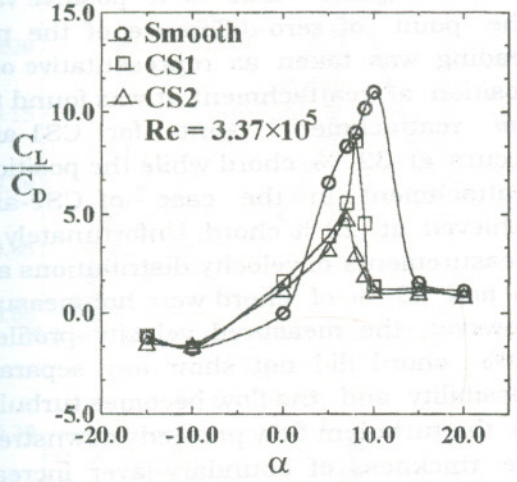

Figure 9 Lift-to-drag ratio of smooth and corrugated airfoils with attack angle

The effect of Reynolds number on the maximum value of lift-to-drag ratio is seen in Figure 10 for corrugated airfoil compared with smooth one. This figure indicates for corrugated surface airfoil that the value of (C_L/C_D) max, which is a measure of maximum airfoil performance, increases with increasing the Reynolds number due to reduced net drag. It is appeared also from Figure 10 that, the maximum lift-to-drag ratio which gives good airfoil performance is strongly dependent upon the surface condition, angle of attack and Reynolds number.

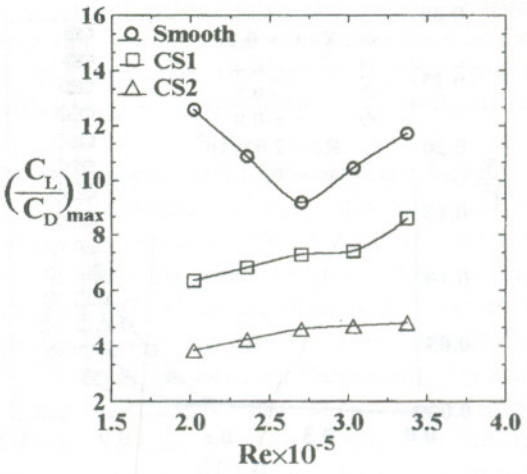

Figure 10 Effect of Reynolds number on the maximum lift-to-drag ratio of smooth and corrugated airfoils

Mean-Velocity Profiles

The mean-velocity profiles of boundary layer development on the smooth and corrugated airfoils are illustrated in Figure 11 at zero-angle of attack and for Reynolds number of 2.02×10^5. The values of local velocity (u) are normalized by the free-stream velocity (U_o) while the value of y-coordinate is normalized by the airfoil chord (C). The measurements of streamwise velocity profiles are conducted at different streamwise airfoil sections, namely X/C=0.1, 0.4, 0.7 and 0.9. Generally, there is an evidence of a strong distortion of the velocity profiles due to the presence of rough corrugations. For zero-angle of attack case, it is seen from Figure 11 that, the maximum velocity is shifted from the free-stream to the wall region of CS1-airfoil. On the contrary, the maximum velocity occurs in the outer flow as the flow approaches the trailing edge, see velocity profile at X/C=0.9. However, the measured velocity profile, which is shown at X/C=0.7 past CS1-airfoil, indicates inflection point in the wall region due to the change from corrugated surface to smooth one. Note that increasing the corrugated length, CS2-airfoil, causes more distortion in the velocity profiles, especially at the leading-edge and near to the trailing-edge.

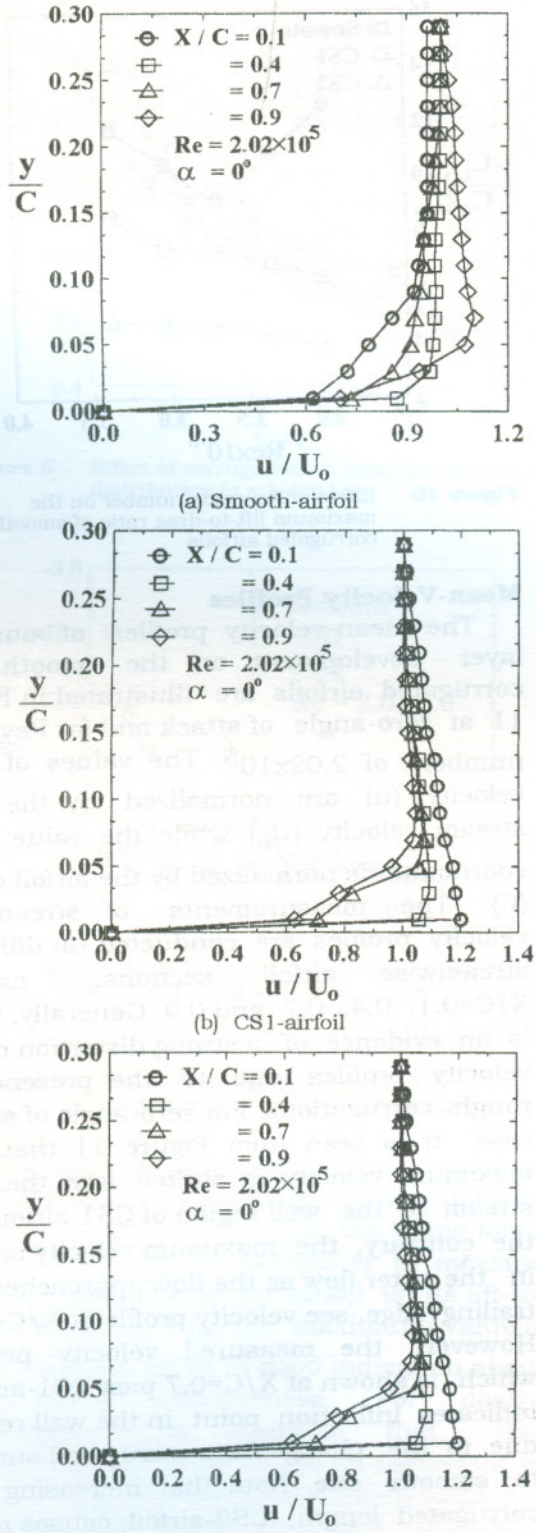

Figure 11 Measured velocity profiles for smooth, CS1 and CS2 airfoils

A remarkable effect of corrugation on the mean-velocity profiles at 10 degrees angle of attack is noticed in Figure 12. Figure 12 shows for 10 degrees angle of attack and for the corrugated airfoils, separation starts to occur at X/C = 0.1, however, at X/C = 0.4 it seems to have disappeared and then reappeared at X/C = 0.7. The experiments were repeated many times to confirm that, the data is free from errors. This may be explained as follows. A laminar separated flow occurs near the leading edges of CS1 and CS2-airfoils (X/C=0.1). The position of reattachment of the separation bubble was determined by traversing the flatted pitot tube along CS1 and CS2-airfoil surfaces. Accordingly, the pitot-readings changed from a negative value to a positive value. The point of zero-difference of the pitot-reading was taken as representative of the position of reattachment. It was found that, the reattachment point for CS1-airfoil occurs at 32 % chord while the position of reattachment in the case of CS2-airfoil achieved at 22 % chord. Unfortunately, the measurements of velocity distributions at 20 % and 30 % of chord were not measured. However, the measured velocity profiles at 40% chord did not show any separation possibility and the flow becomes turbulent. As the turbulent flow proceeds downstream, the thickness of boundary-layer increases and then separation occurs at 70 % of the chord, as shown in Figure 12, and the separated flow extends up to the trailing edge. This results from the reduced momentum transport within the boundary layer. The values of reverse velocities are increased with increasing the length of corrugated surface. The main observation from the measured velocity profiles along the corrugated airfoils is that, the length of separation bubble is reduced with increasing the length of corrugated surface. This means that the extent of laminar region on CS1-airfoil is much more than that of CS2-airfoil. Consequently, the CS2-airfoil subject to earlier separated flow than the

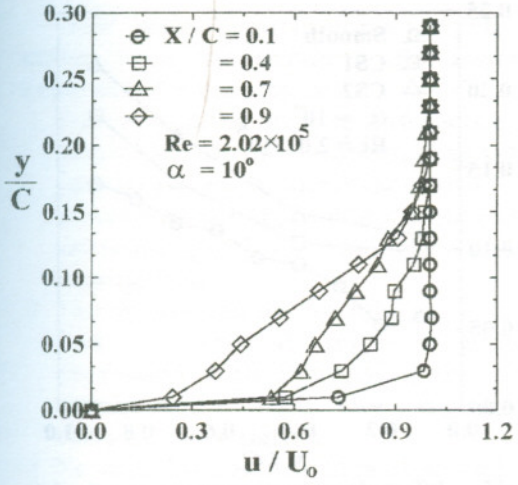

(a) Smooth-airoil

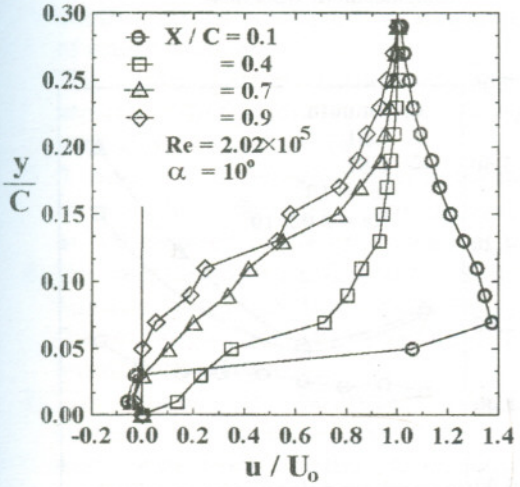

(b) CS1-airfoil

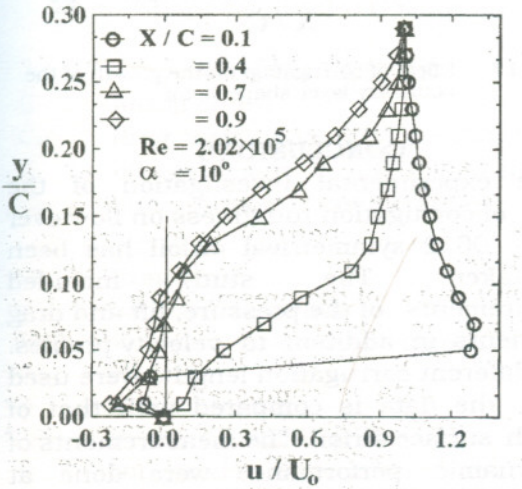

(c) CS2-airfoil

Figure 12 Measured velocity profiles for smooth, CS1 and CS2 airfoils

CS1-airfoil and hence the stalling condition occurs fast. This also explains the reason of decreasing the maximum lift-to-drag ratio with increasing the length of corrugation.

Development of The Boundary Layer

The corresponding development of the boundary layer is illustrated in Figures 13 to 15 at zero-angle of attack and in Figures 16 and 17 at angle of attack of 10 degrees, as measured by the momentum thickness (θ), the displacement thickness (δ^*) and the shape factor (H). For zero-degree angle of attack, it can be seen that the boundary layer getting thicker on the CS2-airfoil than that of smooth and CS1-airfoils. The growth of the shape factor of boundary layer past CS1 and CS2-airfoils at zero-angle of attack did not arrives the separation criteria ($H > 2.4$) near to the leading edge [15]. On the other hand, for 10 degrees angle of attack and as shown in Figures 16 and 17, the results of boundary layer parameters indicate that the shape factor has a value of 2.7 near to the leading edge where the flow is laminar. This value of shape factor lies in the range of separation criteria of laminar flow ($2.5 < H < 3.5$), [14].

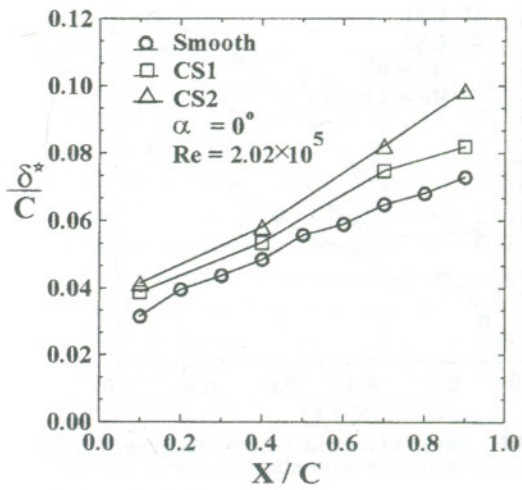

Figure 13 Effect of corrugation on the growth of the displacement thickness

For CS1 and CS2-airfoils and at α=10 degrees, the shape factor of boundary layer decreases up to 40% chord but still has a higher value (H = 2.4). The high value of H towards the trailing edge of corrugated airfoils suggests that the flow may be separate over the airfoil. This may be due to the distorted velocity profiles over the corrugated airfoil and the presence of adverse pressure gradient, as observed in Figure 12.

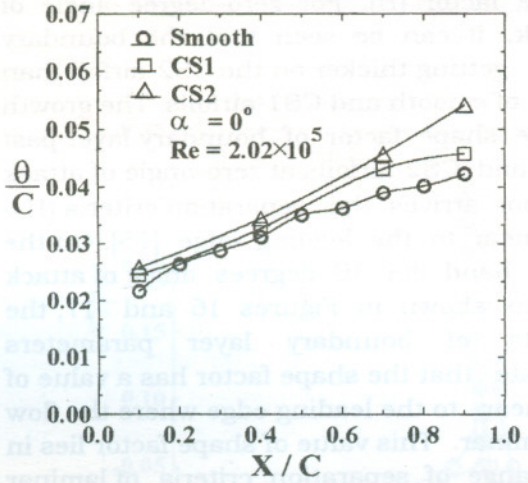

Figure 14 Effect of corrugation on the growth of the momentum thickness

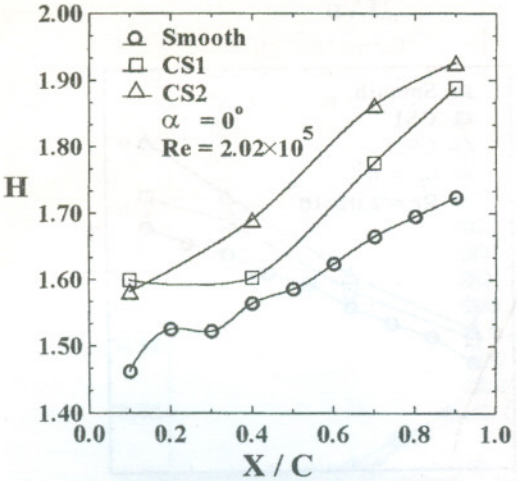

Figure 15 Effect of corrugation on the growth of the boundary layer shape factor

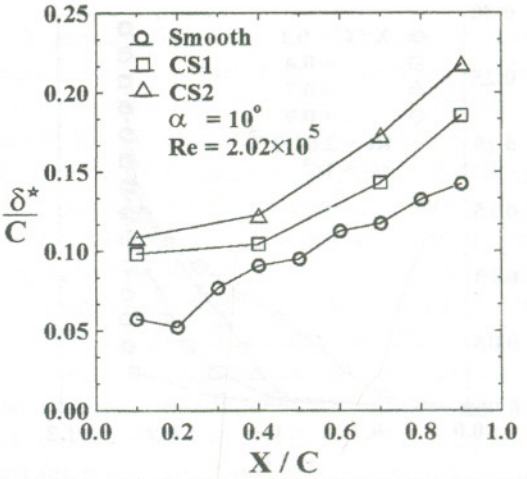

Figure 16 Effect of corrugation on the growth of the displacement thickness

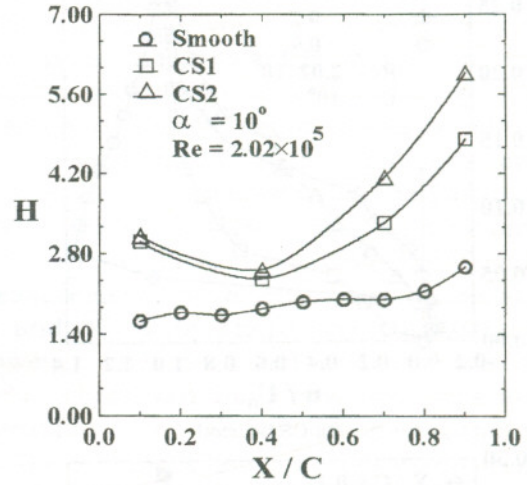

Figure 17 Effect of corrugation on the growth of the boundary layer shape factor

CONCLUSIONS

An experimental investigation of the effect of corrugation roughness on flow over NACA- 0012 symmetrical airfoil has been undertaken. The study included measurements of the pressure, lift and drag coefficients in addition to velocity profiles. Two different corrugation lengths were used where the data is compared with that of smooth surface airfoil. The measurements of aerodynamic performance were done at different Reynolds number.

The main conclusions which can be drawn from the pervious discussion of the experimental results are :

1. For corrugated surface airfoils the maximum lift-to-minimum drag ratio of corrugated airfoil increases with increasing the Reynolds number and decreasing with increasing the length of corrugation.
2. The maximum lift-to- minimum drag ratio and the critical angle of attack are decreased with increasing the length of corrugation within the range of tested corrugation lengths.
3. No-zero lift coefficient is observed at zero-angle of attack, but the zero-lift coefficient is occurred at negative value of angle of attack.
4. The corrugation roughness causes a strong distortion of the downstream turbulent boundary layer.
5. A laminar separation flow is formed near to the leading edge of corrugated airfoils at 10 degrees angle of attack.
6. The reattachment point of the separated laminar boundary layer moves towards the leading edge with increasing the length of corrugation.
7. The turbulent boundary layer past corrugated airfoils grows more rapidly and separates earlier than that the smooth airfoil. This is seen in the values of the shape factor of the boundary layer.

NOMENCLATURE

C	airfoil chord
C_D	drag coefficient, $D/(0.5\,\rho\,U_o^2\,C)$
C_L	lift coefficient, $L/(0.5\,\rho\,U_o^2\,C)$
C_P	static-pressure coefficient, $(P - P_o)/(0.5\,\rho\,U_o^2)$
D	drag force
d	corrugation depth
H	boundary layer shape factor, δ^*/θ
L	lift force
P	static pressure
Re	Reynolds number, $U_o\,C/\nu$
S	corrugation wave pitch
U_o	free-stream velocity
u	fluid-velocity parallel to airfoil surface
X	streamwise-direction along the chord line, with origin at the leading edge
y	crosswise-direction normal to the chord line
α	angle of attack
δ	boundary layer thickness, value of y at which $u = 0.99\,U_o$
δ^*	boundary layer displacement thickness, $\int_0^{\delta} (1-\frac{u}{U_o})\,dy$
θ	boundary layer momentum thickness, $\int_0^{\delta} (1-\frac{u}{U_o})\,\frac{u}{U_o}\,dy$
ν	kinematic viscosity

Subscripts

min	minimum conditions
max	maximum conditions
o	free-stream value
cr	critical condition

REFERENCES

1. P.S. Klebanoff, G.B. Schubauer and K.D. Tidstrom, "Measurements of the Effect of Two and Three-Dimensional Roughness Elements on Boundary Layer Transition", J. Aero Sci, Vol. 22, pp. 803, (1955).
2. B.H. Carmichael, "Critical Reynolds number for Multiple Three-Dimensional Roughness Elements", Northrop Aircraft Report No. NAI- 58-589 (BLC-112) (1958).
3. L.K. Loftin, "Effects of Specific Types of Surface Roughness on Boundary-Layer Transition", NACA Report No. L - 48, (1948).
4. J.C. Gibbings, O.T. Goxel and D.J. Hall, "The Influence of Roughness Trips Upon Boundary-Layer Transition", Part 2: Characteristics of Single Spherical Trips". The Aero. Journal, 90, pp. 357, (1986).
5. J.C. Gibbings, O.T. Goxel and D.J. Hall, "The Influence of Roughness Trips Upon Boundary-Layer Transition", Part 3: Characteristics of Rows of Spherical Transition Trips". The Aero. Journal, Vol. 91, pp. 393, (1986).
6. A. Fage, "The Smallest Size of Spanwise Surface Corrugation which Affects Boundary Layer Transition on an Airfoil ",

Aeronautical Research Council, R & M 2120, (1943).
7. R.E Brumby, "Wing Surface Roughness Cause an Effect", DC Flight Approach, pp. 2, (1979).
8. M.B. Bragg and G.M. Georgerek, "Aerodynamic Characteristics of Airfoil with Ice Accretions" , AIAA paper 82 - 0282, (1982).
9. K.D. Korkan, E.J. Cross Jr. and C-C. Cornell, "Experimental Aerodynamic Characteristics of an NACA - 0012 Airfoil with Simulated Ice", Aircraft Journal, Vol. 22, pp. 130, (1986).
10. H.A. Abdalla, A. M. Alam El-Din, T. I. Sabry and S. R. Ismail, "Aerodynamic Performance and Boundary Layer Growth on Rough Symmetrical Airfoil at Low - Reynolds Number", Alexandria Engineering. Journal, Vol. 36, No. 3, pp. A155, (1997).
11 Wanmin Gong, Peter A. Taylor and Andreas Dornbrack, "Turbulent Boundary-Layer Flow Over Fixed Aerodynamically Rough Two-Dimensional Sinusoidal Waves", J. Fluid Mech., Vol. 312, pp. 1-37, (1996).
12. J.C. Han, J.S. Park and C.K. Lei, "Heat Transfer Enhancement in Channels with Turbulence Promoters", Trans. ASME, J. of Engineering for Gas Turbines and Power, Vol. 107, pp. 628-635, (1985).
13. S.J. Kline and F.A. Mcclintock, "Describing the Uncertainties in Single-Sample Experiments", ASME, Mechanical Engineering Journal, pp. 3, (1953).
14. I.H. Abbott and A.E. Von Doenhoff, "Theory of Wing Sections", Dover publications, INC., New York, (1949).
15. H. Schlichting, "Boundary Layer Theory", 6th ed., Mc Graw - Hill. New York., (1968).

Received December 18, 1997
Accepted June 25, 1998

نمو الطبقة المتاخمة على سطوح انسياب هوائية ناعمة ومموّجة

حسن عوض عبد اللـــه ، عاطف علم الدين ، طاهر إبراهيم صبرى ، صابر إسماعيل
قسم هندسة القوى الميكانيكيه – جامعة المنوفيه

ملخص البحث

يتناول هذا البحث دراسة معملية لدراسة تأثير الخشونة الناتجة من تموج السطوح التى تتبع دالة الجيب علـــى الخصـــائص الإيروديناميكيه ونمو الطبقة المتاخمة على الإيروفيل المتماثل.

فى هذا البحث ، تم إجراء دراسة معمليه لتأثير مثل هذا النوع من الخشونة على معامل الرفع ومعامل المقاومة عند زوايـــا هجوم مختلفه ، رقم الرينولدز ، وأطوال مختلفه للسطح المموج. كذلك تم إجراء قياسات لتوزيع الضغوط الإســـتاتيكيه وتوزيـــع السرعات عند زوايا هجوم مختلفة وتم حساب البارامترات المختلفة للطبقة المتاخمة فى حالة وجود تدرج موجب للضغط وفى حالة عدم وجود تدرج للضغط.

وقد أظهرت النتائج المعملية لهذا البحث أن زاوية الهجوم الحرجة وأقصى أداء لمثل هذه السطوح (الذى يقاس كنسبه بين معاملى الرفع والمقاومة) يزيد بزيادة رقم الرينولدز ويقل بزيادة طول السطح المموج. كذلك بينت النتائج وجود تشوه فى توزيع السرعات نتيجة لوجود تموج بالسطح مما أدى إلى نمو سريع للطبقة المتاخمة ، مما ترتب عليه حدوث إنفصال مبكـــر للســـريان فى منطقى السريان الرقائقى والإضطرابى مقارنة بالسطوح الناعمة. وقد وجد أيضا أن السطوح المموجة تغير من قيمة زاوية الهجوم التى يصبح عندها معامل الرفع مساويا للصفر.